SUPPLEMENTAL INFORMATION

Figure S1, related to Figure 1: Hierarchical clustering of normalized mouse metabolome data

(A) Color Heat map showing the fold change of the 129 metabolites identified by mass spectrometry analysis from biological triplicate samples of the 9.5 day mouse embryo posterior body region shown in Figure 1A. Each data point is normalized to the mean value of all triplicate samples. Hierarchical clustering of triplicate P-PSM, A-PSM samples, and 2 somite samples using Pearson correlation coefficient. Dotted red box highlights glycolysis metabolites.

(B) Box plots graph of the metabolites associated to glycolysis detected in the metabolomics analysis (* Significant at $p<0.05$ with t-test).

Figure S2, related to Figure 2: Generation of gene expression profiles in the chicken PSM differentiation microarray series

Histograms representing expression profiles of transcripts detected in the microarray series of chicken embryo posterior paraxial mesoderm described in Figure 2. The histograms were generated from MAS expression value for a given probeset, with samples of the two microdissection series arranged according to their position along the antero-posterior axis (posterior to the left) as described in Chal et al. (2015). The resulting profile gives a quantitative view of transcript expression during early stages of paraxial mesoderm differentiation.

Expression of representative genes associated to major signaling pathways involved in PSM patterning and differentiation is shown. "Posterior" signaling pathway genes are highlighted by a Green box, and Blue box represent genes for anterior signaling pathways. Orange box show genes preferentially expressed at the determination front. Notch signaling pathway components including cyclic genes are highlighted by a Black box. Bottom: schematic representation of the signaling

gradients and of the major posterior paraxial mesoderm domains (color-coded) . Orange bar marks the determination front level where cells acquire their segmental identity.

Figure S3, related to Figure 4: Axial elongation defects caused by glucose starvation are independent of cell proliferation and apoptosis

2-day old chicken embryos cultured 3h on a DMEM-based plate with 0.15% glucose (A, C), or without glucose (B, D), stained in whole mount with phosphorylated histone H3 (pH3, green) showing proliferating cells (A n=6, B n=6), and with lysotracker staining (red) for apoptotic cells (C n=9, D n=9). Nuclei are labeled in blue with DAPI in (A, B). Ventral views, anterior to the top. Scale bar :100 µm. Asterisk indicate newly formed somites and arrowheads indicate tail bud region.

Figure S4, related to Figure 5: Effect of pH increase on elongation

(A, B) Expression dynamics of two different probesets of *MMP2* in the tail bud and posterior PSM as detected in the chicken microarray series.

(C, D) Elongation time course of 2-day chicken embryos cultured on a control EC plate (C: pH 9.6) and on an alkaline plate (D : pH11.0). Bright field micrographs of the posterior region taken at 1.5 hour intervals. Somites formed at the last time point are indicated by asterisks on the right. Ventral views, anterior to the top.

(E-H) Whole mount *in situ* hybridization of 2-day chicken embryos with probes for (*T*/*BRACHYURY*) (E: n=3, G: n=3) and ***CMESPO*** (F: n=3, H: n=3), after 6 hr culture in a control plate (E, F: pH 9.6) and in alkaline plate (G: n=3, H: n=3: pH11.0) . Ventral view, anterior to the top.

Figure S5, related to Figure 6: Axial elongation defects caused by glycolysis inhibition are independent of cell proliferation and apoptosis

(A-H) 2-day old chicken embryos stained in whole mount with phosphorylated histone H3 (pH3, green) for proliferating cells, and with TUNEL staining (magenta) for apoptotic cells. Nuclei are labeled with DAPI (blue). Control (A-C, n=4), 2DG (B-F, n=4), NaN3-treated embryo (F-H, n=4). Ventral views, anterior to the top. Scale bar :100 µm. Asterisk indicate newly formed somites, and arrowheads indicate tail bud region.

(C, F, H) Higher magnification of the panels shown in A-G showing the tail bud region. Dashed boxes show areas where proliferation and apoptosis were analyzed in the tailbud region (yellow line), the PSM region (white line) and the lateral plate mesoderm region (grey line). Scale bar :100 µm.

(I-J) Histograms showing the corresponding quantification of cell proliferation (I) and apoptosis (J) by mesoderm regions and by treatments. Data represent four independent experiments with error bars ± SD. Statistical significance was assessed with one way ANOVA followed by Tukey's test (*P<0.05 , ****P<0.0001, ns P>0.05).

Table S1, related to Figure 1: Raw data of the metabolomic experiment.

Table S2, related to Figure 1: Expression Fold change of Glycolysis genes along the Paraxial mesoderm in a 9.5 day mouse embryo

Fold changes of expression levels of Glycolysis genes shown in Figure 1H along the Paraxial mesoderm in 9.5 day old mouse embryo. Expression fold changes along the paraxial mesoderm domains correspond to ratios of normalized MAS values. Posterior Domain corresponds to the average of TB1, PSM1, PSM2 fragments while the Anterior Domain corresponds to an average of the fragments PSM3, PSM4, PSM5. Tailbud corresponds to TB1 fragments. A-PSM corresponds to PSM4, PSM5 fragments. Statistical significance was determined with an unpaired Student-test with the following cutoffs: ns $p>0.05$, *$p<0.05$, **$p<0.01$, ***$p<0.001$,****$p<0.0001$.

Table S3, related to figure 2: Expression Fold change of Glycolysis genes along the Paraxial mesoderm in a 2-day old chicken embryo

Fold changes of expression levels of Glycolysis genes along the paraxial mesoderm in Stage 12HH chicken embryo. Expression fold changes along paraxial mesoderm domains corresponds to ratios of normalized MAS values. Posterior Domain corresponds to the average of (TB1, PSM1, PSM2, PSM3) while the Anterior Domain corresponds to an average of fragments (PSM4, PSM5, PSM6, PSM7, PSM8). Tailbud corresponds to (TB1) fragments. A-PSM corresponds to (PSM6, PSM7, PSM8). Statistical significance was determined with an unpaired Student-test with the following cutoffs: ns $p>0.05$, *$p<0.05$, **$p<0.01$, ***$p<0.001$,****$p<0.0001$.

Supplemental Movie Legends:

Movie S1, related to Figure 4E-G: Elongation of the embryo in control, 2DG and NaN3 conditions.

Movie S2, related to Figure 5 D-F: Bright field (left) and corresponding cell trajectories of PSM cells electroporated with an H2B-Venus (nuclear) construct (right) are shown for each condition. Only a portion of the trajectories are shown for clarity. The starting time of the movie corresponds to the time when the analysis was started.

Movie S3, related to Figure 5 I-K: Elongation of the embryo in chemically-defined medium with 0.15% glucose and without glucose. Bright field (left) and corresponding cell trajectories of PSM cells electroporated with an H2B-Venus (nuclear) construct (right) are shown for each condition. Only a portion of the trajectories are shown for clarity. The starting time of the movie corresponds to the time when the analysis was started.

Movie S4, related to Figure 5 O-Q: Elongation of the embryo in control and alkaline conditions. Bright field (left) and corresponding cell trajectories of PSM cells electroporated with an H2B-Venus construct (right) are shown for each condition. The starting time of the movie corresponds to the time when the analysis was started.

Movie S5, related to Figure 6: Effect of 2DG on the differentiation of the neuro-mesodermal precursors (NMPs). H2B-RFP was electroporated in the anterior primitive streak area containing the NMPs of stage 4-5HH control (left) and 2DG-treated chicken embryos (right). In the control embryo, electroporated NMPs produce descendants in the neural tube and in the paraxial

mesoderm. In contrast, 2DG treatment inhibits the production of paraxial mesoderm cells while NMP descendants accumulate in the Neural Tube. Dorsal views, anterior to the top.

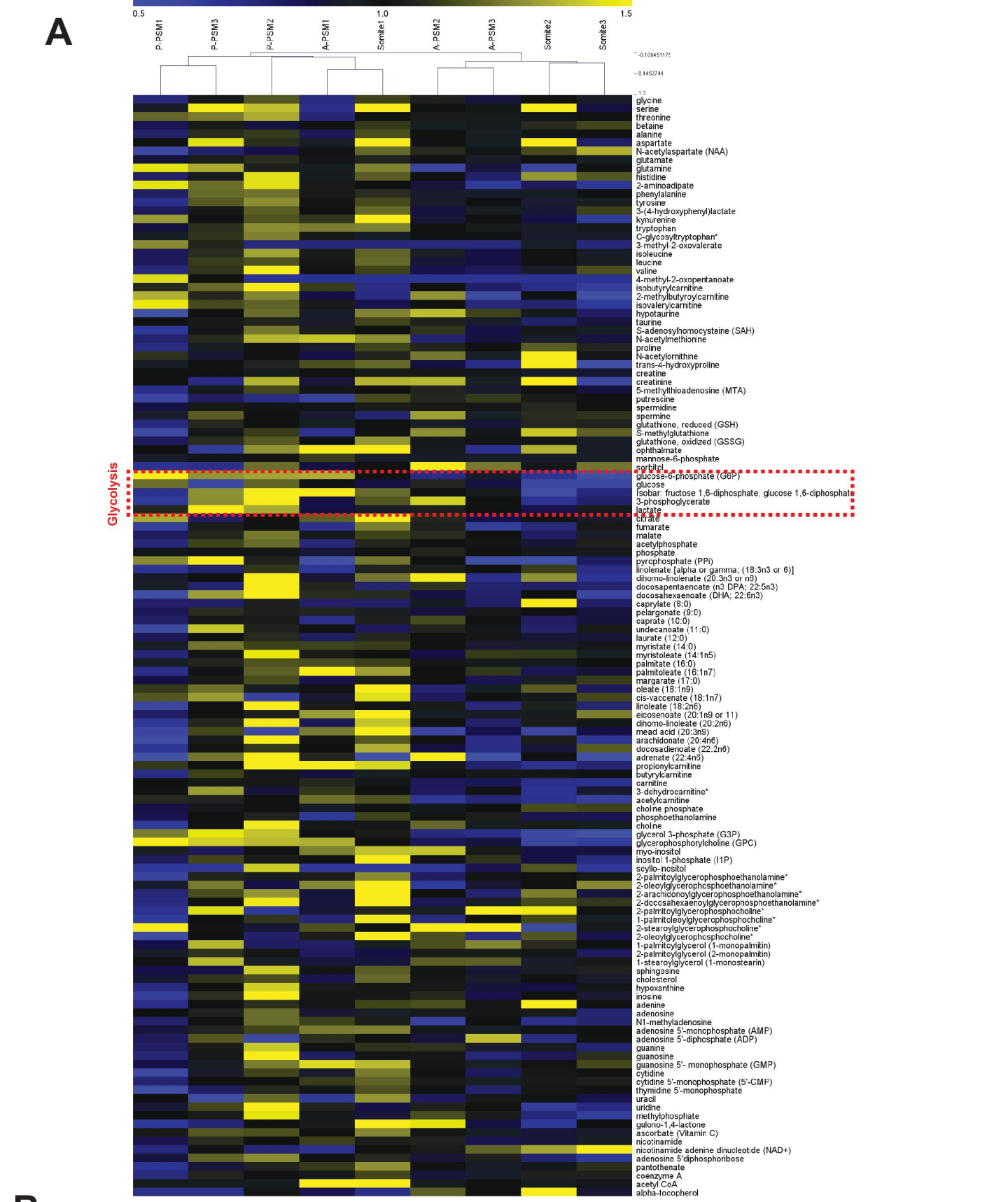
A
0.5
1.0
1.5
P-PSM1
P-PSM3
P-PSM2
A-PSM1
Somite1
A-PSM2
A-PSM3
Somite2
Somite3
glycine
serine
threonine
betaine
alanine
aspartate
N-acetylaspartate (NAA)
glutamate
glutamine
histidine
2-aminoadipate
phenylalanine
tyrosine
3-(4-hydroxyphenyl)lactate
kynurenine
tryptophan
C-glycosyltryptophan*
3-methyl-2-oxovalerate
isoleucine
leucine
valine
4-methyl-2-oxopentanoate
isobutyrylcarnitine
2-methylbutyroylcarnitine
isovalerylcarnitine
hypotaurine
taurine
S-adenosylhomocysteine (SAH)
N-acetylmethionine
proline
N-acetylornithine
trans-4-hydroxyproline
creatine
creatinine
5-methylthioadenosine (MTA)
putrescine
spermidine
spermine
glutathione, reduced (GSH)
S-methylglutathione
glutathione, oxidized (GSSG)
ophthalmate
mannose-6-phosphate
sorbitol
glucose-6-phosphate (G6P)
glucose
Isobar: fructose 1,6-diphosphate, glucose 1,6-diphosphate
3-phosphoglycerate
lactate
citrate
fumarate
malate
acetylphosphate
phosphate
pyrophosphate (PPi)
linolenate [alpha or gamma; (18:3n3 or 6)]
dihomo-linolenate (20:3n3 or n6)
docosapentaenoate (n3 DPA; 22:5n3)
docosahexaenoate (DHA; 22:6n3)
caprylate (8:0)
pelargonate (9:0)
caprate (10:0)
undecanoate (11:0)
laurate (12:0)
myristate (14:0)
myristoleate (14:1n5)
palmitate (16:0)
palmitoleate (16:1n7)
margarate (17:0)
oleate (18:1n9)
cis-vaccenate (18:1n7)
linoleate (18:2n6)
eicosenoate (20:1n9 or 11)
dihomo-linoleate (20:2n6)
mead acid (20:3n9)
arachidonate (20:4n6)
docosadienoate (22:2n6)
adrenate (22:4n6)
propionylcarnitine
butyrylcarnitine
carnitine
3-dehydrocarnitine*
acetylcarnitine
choline phosphate
phosphoethanolamine
choline
glycerol 3-phosphate (G3P)
glycerophosphorylcholine (GPC)
myo-inositol
inositol 1-phosphate (I1P)
scyllo-inositol
2-palmitoylglycerophosphoethanolamine*
2-oleoylglycerophosphoethanolamine*
2-arachidonoylglycerophosphoethanolamine*
2-docosahexaenoylglycerophosphoethanolamine*
2-palmitoylglycerophosphocholine*
1-palmitoleoylglycerophosphocholine*
2-stearoylglycerophosphocholine*
2-oleoylglycerophosphocholine*
1-palmitoylglycerol (1-monopalmitin)
2-palmitoylglycerol (2-monopalmitin)
1-stearoylglycerol (1-monostearin)
sphingosine
cholesterol
hypoxanthine
inosine
adenine
adenosine
N1-methyladenosine
adenosine 5'-monophosphate (AMP)
adenosine 5'-diphosphate (ADP)
guanine
guanosine
guanosine 5'- monophosphate (GMP)
cytidine
cytidine 5'-monophosphate (5'-CMP)
thymidine 5'-monophosphate
uracil
uridine
methylphosphate
gulono-1,4-lactone
ascorbate (Vitamin C)
nicotinamide
nicotinamide adenine dinucleotide (NAD+)
adenosine 5'diphosphoribose
pantothenate
coenzyme A
acetyl CoA
alpha-tocopherol
Glycolysis
B
Glucose
Glucose-6-phosphate (G6P)
Fructose-1,6-diphosphate (FBP)
3-phosphoglycerate
lactate
glutamine
P-PSM
A-PSM
Somite

Figure S1

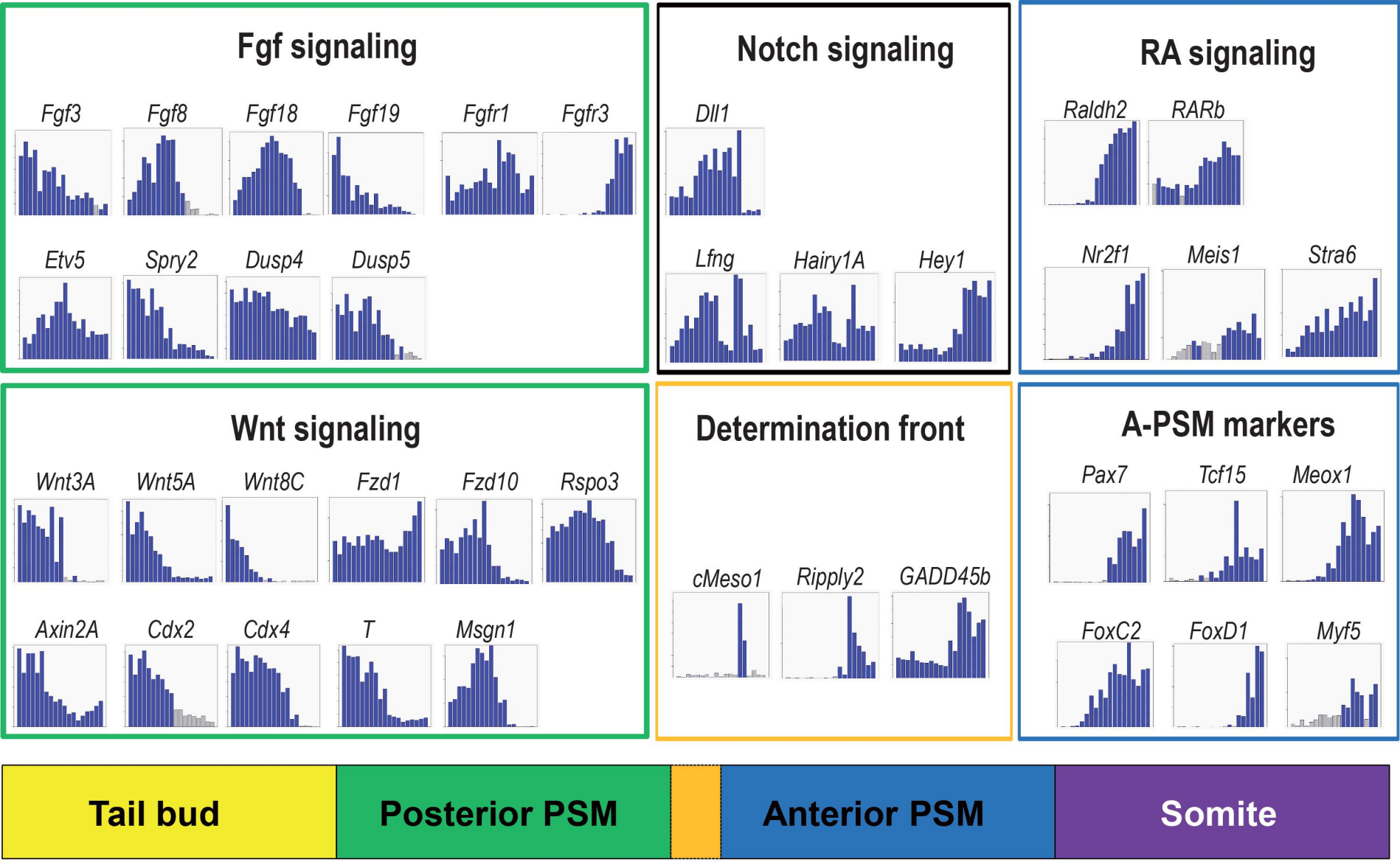
Fgf signaling
Fgf3
Fgf8
Fgf18
Fgf19
Fgfr1
Fgfr3
Etv5
Spry2
Dusp4
Dusp5
Notch signaling
Dll1
Lfng
Hairy1A
Hey1
RA signaling
Raldh2
RARb
Nr2f1
Meis1
Stra6
Wnt signaling
Wnt3A
Wnt5A
Wnt8C
Fzd1
Fzd10
Rspo3
Axin2A
Cdx2
Cdx4
T
Msgn1
Determination front
cMeso1
Ripply2
GADD45b
A-PSM markers
Pax7
Tcf15
Meox1
FoxC2
FoxD1
Myf5
Tail bud
Posterior PSM
Anterior PSM
Somite

Figure S2

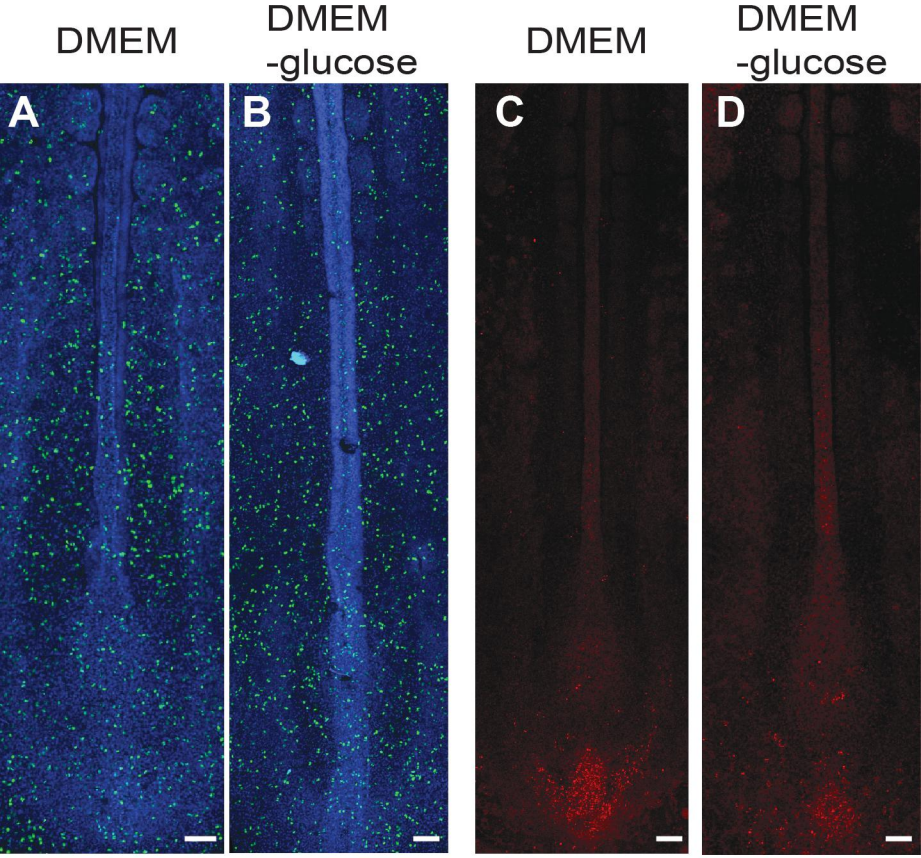

Figure S3

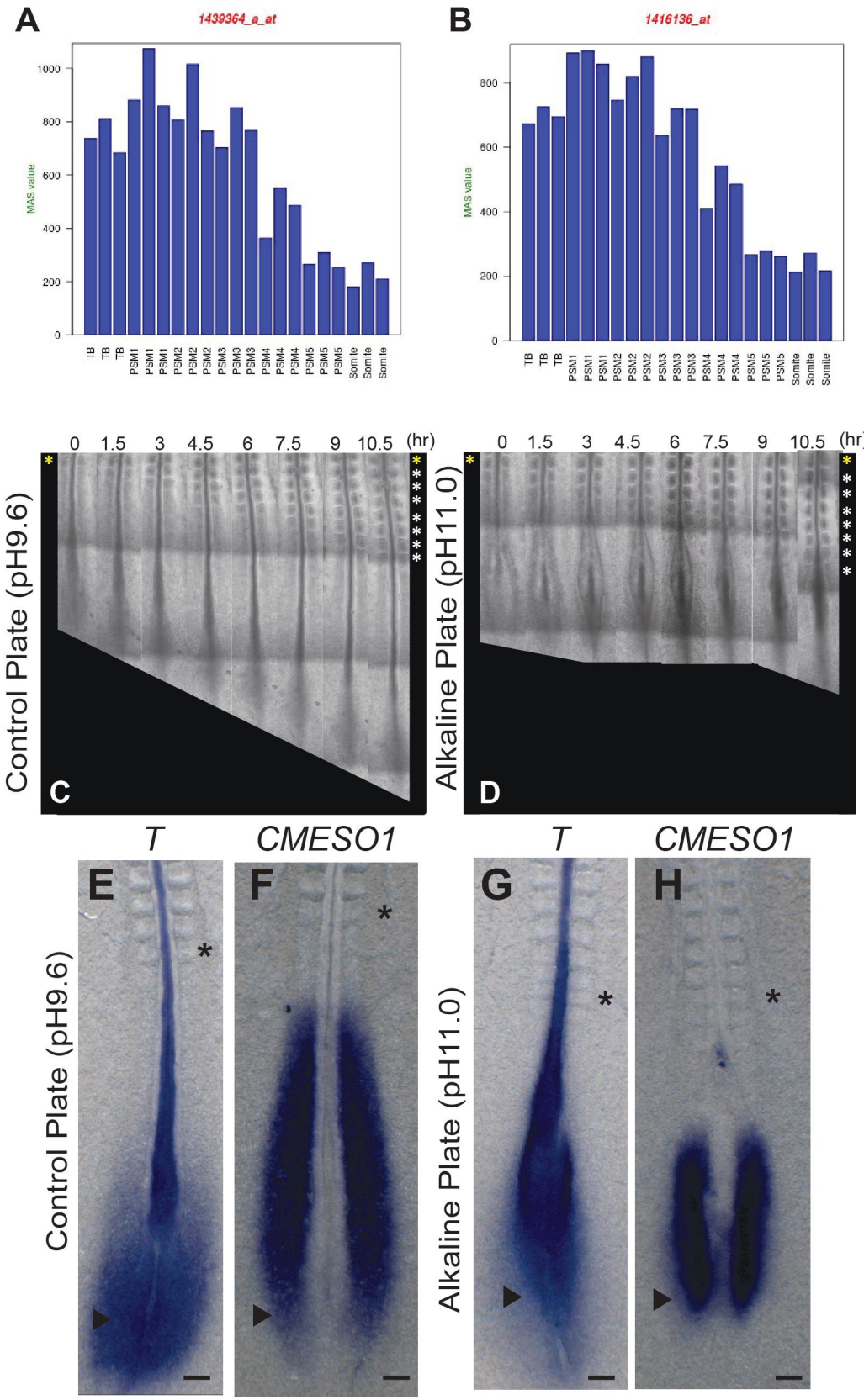
A
1439364_a_at
MAS value
1000
800
600
400
200
0
TB
TB
TB
PSM1
PSM1
PSM1
PSM2
PSM2
PSM2
PSM3
PSM3
PSM3
PSM4
PSM4
PSM4
PSM5
PSM5
PSM5
Somite
Somite
Somite
B
1416136_at
MAS value
800
600
400
200
0
0
1.5
3
4.5
6
7.5
9
10.5
(hr)
Control Plate (pH9.6)
C
Alkaline Plate (pH11.0)
D
T
CMESO1
E
F
G
H
Control Plate (pH9.6)
Alkaline Plate (pH11.0)

Figure S4

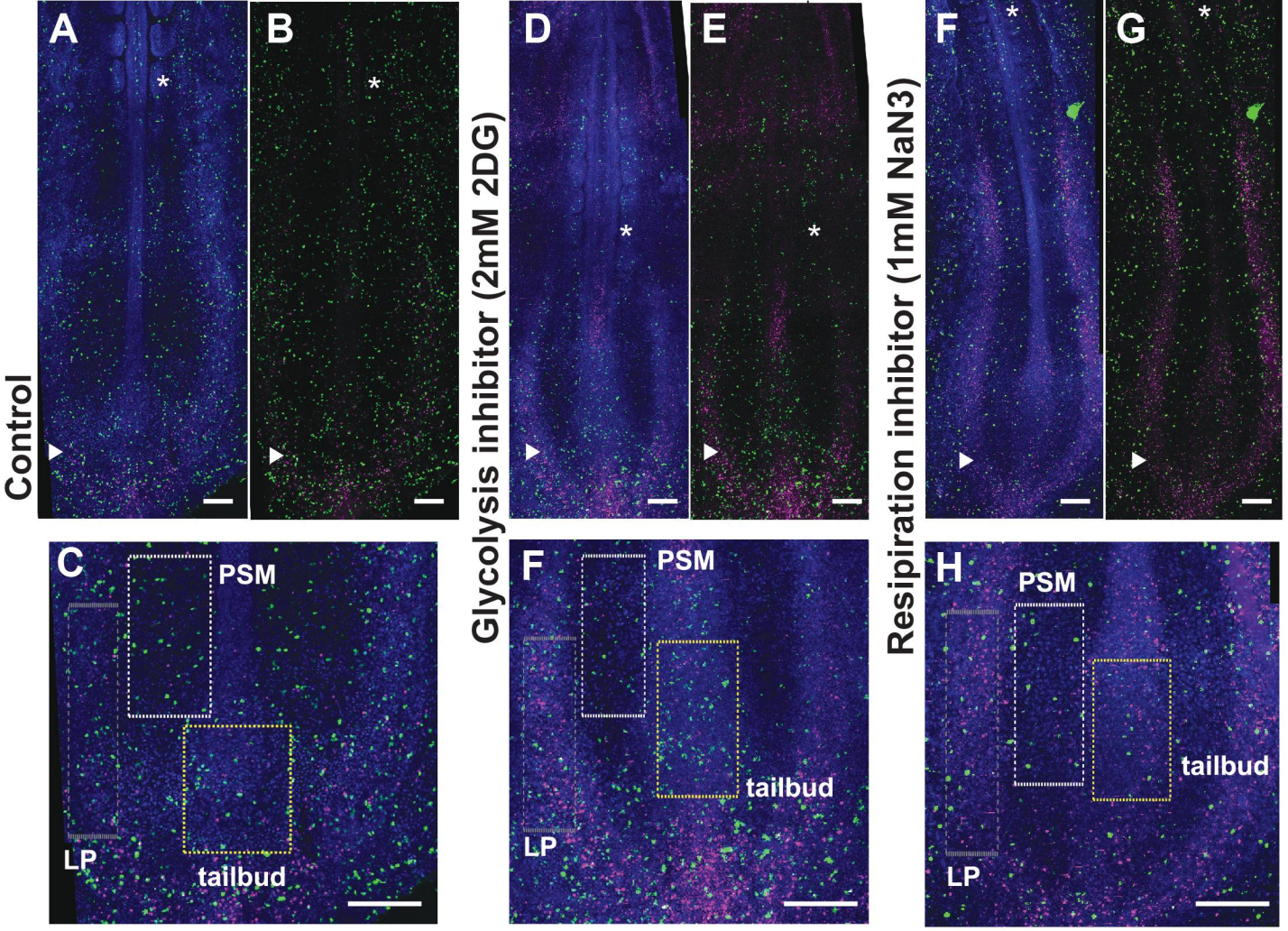
A
B
D
E
F
G
Control
Glycolysis inhibitor (2mM 2DG)
Resipiration inhibitor (1mM NaN3)
C
PSM
LP
tailbud
F
PSM
tailbud
LP
H
PSM
tailbud
LP

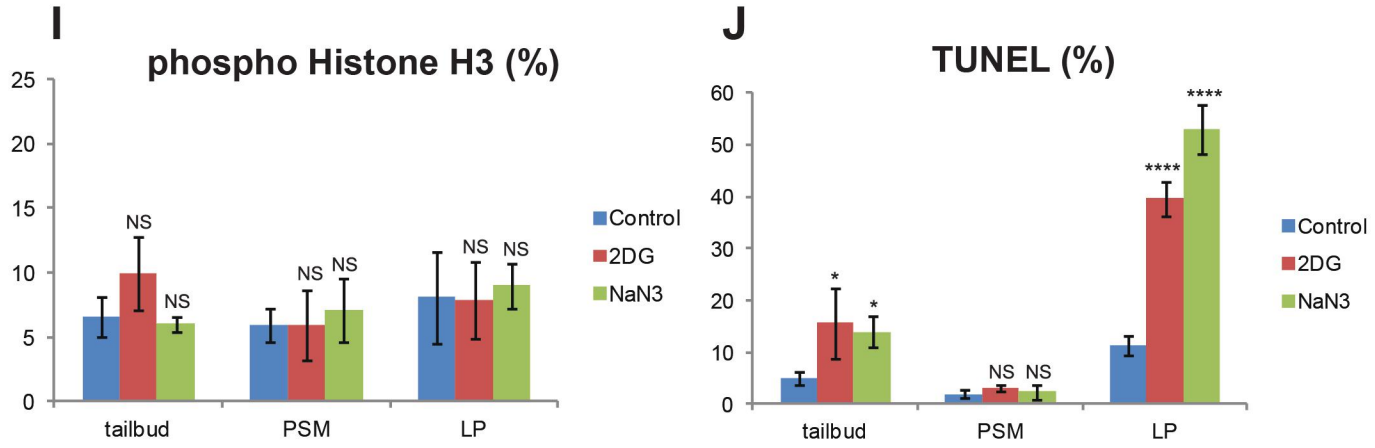
I
phospho Histone H3 (%)
25
20
15
10
5
0
NS
NS
NS
NS
NS
NS
tailbud
PSM
LP
Control
2DG
NaN3
J
TUNEL (%)
60
50
40
30
20
10
0
*
*
NS
NS
****
****
tailbud
PSM
LP
Control
2DG
NaN3

Figure S5

Table S2: Expression Fold change of Glycolysis genes along the paraxial mesoderm in 9.5 day old mouse embryo

		Posterior /Anterior		Tail bud/A-PSM	
Gene symbol	Affymetrix Probe ID	Fold change	P-value	Fold change	P-value
Slc2a3	1437052_s_at	3.59	**	7.55	**
Slc2a3	1455898_x_at	4.95	*	11.02	**
Pgm1	1453283_at	1.91	***	2.59	****
Pgm2	1451149_at	1.39	ns	2.06	**
HK1	1437974_a_at	1.20	ns	1.31	ns
Aldoa	1433604_x_at	1.12	ns	1.39	***
Aldoa	1434799_x_at	1.09	ns	1.30	**
Tpi1	1415918_a_at	0.99	ns	1.14	ns
Bpgm	1415864_at	2.05	**	3.25	***
Bpgm	1415865_s_at	1.93	***	2.87	**
Eno3	1417951_at	1.69	*	1.27	**
LDHB	1448237_x_at	1.30	*	1.39	ns
LDHB	1455235_x_at	1.32	*	1.38	ns

Expression fold changes along Paraxial mesoderm domains corresponds to ratios of normalized MAS values.
Posterior Domain corresponds to the average of TB1, PSM1, PSM2 fragments while the Anterior Domain corresponds to an average of fragments PSM3, PSM4, PSM5
Tail bud corresponds to TB1 fragments
A-PSM corresponds to PSM4, PSM5 fragments.
Statistical significance was determined with an unpaired Student-test with the following cutoffs: ns P>0.05, *P<0.05 , **P<0.01, ***P<0.001,****P<0.0001

Table S3: Expression Fold change of Glycolysis genes along the Paraxial mesoderm in stage 11HH chicken embryo

		Posterior/Anterior		Tail bud/A-PSM	
Gene symbol	Affymetrix Probe ID	Fold change	P-value	Fold change	P-value
SLC2A1	Gga.1040.1.S1_at	1.66	**	1.25	ns
HK1	Gga.2197.1.S1_s_at	1.37	**	1.50	ns
Gpi1	GgaAffx.20134.1.S1_s_at	1.97	**	2.57	**
PFKFB4	GgaAffx.25392.2.S1_s_at	1.36	ns	1.59	ns
PFKP	Gga.5753.1.S1_s_at	1.35	**	1.61	*
G3P	Gga.1374.4.S1_x_at	1.09	*	1.18	*
PGK1	Gga.4503.1.S1_a_at	1.45	**	1.74	*
PGAM1	Gga.6033.1.S1_s_at	1.33	*	1.35	ns
ENOA	Gga.1383.1.S1_at	1.14	**	1.24	*
PKM	Gga.4299.1.S1_at	1.34	***	1.45	*
LDHB	Gga.4149.1.S1_at	1.42	****	1.66	***

Expression fold changes along Paraxial mesoderm domains corresponds to ratios of normalized MAS values.
Posterior Domain corresponds to the average of (TB1,PSM1,PSM2,PSM3)
while the Anterior Domain corresponds to an average of fragments (PSM4,PSM5,PSM6,PSM7,PSM8)
Tail bud corresponds to (TB1) fragments
A-PSM corresponds to (PSM6,PSM7,PSM8)
Statistical significance was determined with an unpaired Student-test with the following cutoffs: ns P>0.05, *P<0.05 , **P<0.01, ***P<0.001,****P<0.0001